

A Comparison of the Performance of 3-5 and 8-12 μm Infrared Cameras

Thomas Meitzler
Grant Gerhart
Euijung Sohn
Paul Collins

US Army TARDEC
Survivability Tech Center
Research Group
Warren, MI 48397-5000

Abstract

An image based comparison of modeled infrared cameras in the medium-wave (MW) and longwave (LW) bands is done using the TARDEC Thermal Image Model (TTIM) and LOWTRAN7. A state-of-the-art staring focal plane array (FPA), a common module scanning FLIR, and a scanning dual-band sensor are modeled. The simulations using TTIM demonstrate the imaging performance of the cameras as well as the degradation caused by the atmosphere in the two bands. Atmospheric degradation to the image is simulated in rain and fog in northern hemisphere environments.

1. Introduction

For a particular scenario, the question often arises, what is the optimum waveband for remote infrared (IR) detection by a sensor? This question is important to the Army for the simulation of thermal target signatures and the effects of signature suppression on acquisition ranges of infrared sensors. Many studies¹⁻⁴ have been done to assess the relative performance of 3-5 micron and 8-12 micron systems. Previous studies often produced conflicting results. Variables that effect the actual and simulated performance of the imaging sensor are: the size of the target, path length through the atmosphere, the atmospheric transmission model used, and the detector system technology. As is to be expected, many of these parameters change with time due to advances in both the sensor materials and architecture as well as the model fidelity. Most of the previous studies have used some version of LOWTRAN to model the atmospheric effects on the image. Since the early studies by Tauer¹ with LOWTRAN3, the LOWTRAN code has been enhanced to calculate atmospheric radiance in the presence of altitude and humidity dependent aerosols, water vapor continuum absorption models have been added, and aerosol back scattering included. Recently, LOWTRAN7 has been incorporated into MODTRAN. MODTRAN is a upgraded version of LOWTRAN that has a resolution of one micron to 20 microns, whereas the highest resolution LOWTRAN can obtain is five microns. MODTRAN was used by the authors to verify the case studies that were analyzed by TTIM and LOWTRAN.

Previous studies have gauged system performance on the SNR vs. range or the detectivity (D^*) vs. wavelength. The contribution the authors make to the literature on this topic is a image for the several comparison case studies. The computer model used for this study is the TACOM Thermal Image Model (TTIM)⁷ TTIM historically is an extension of the NVL Model by Ratches.⁸ TTIM can model the sensor degradation to an image in any of the IR bands. See Figure 1 for a schematic of the scanning and focal plane array (FPA) sensor modeling methodologies. The scene radiance map is adjusted for atmospheric and battlefield effects (TTIM calls LOWTRAN7 for the calculation of transmittance, path radiance, and the extinction coefficient), then the received power map is converted into the frequency domain by a Fast Fourier Transform (FFT). Next, atmospheric and system optical MTF's are convolved and the then the inverse FFT taken to produce a sensor signal output map which is then converted to an output image.

Report Documentation Page

Form Approved
OMB No. 0704-0188

Public reporting burden for the collection of information is estimated to average 1 hour per response, including the time for reviewing instructions, searching existing data sources, gathering and maintaining the data needed, and completing and reviewing the collection of information. Send comments regarding this burden estimate or any other aspect of this collection of information, including suggestions for reducing this burden, to Washington Headquarters Services, Directorate for Information Operations and Reports, 1215 Jefferson Davis Highway, Suite 1204, Arlington VA 22202-4302. Respondents should be aware that notwithstanding any other provision of law, no person shall be subject to a penalty for failing to comply with a collection of information if it does not display a currently valid OMB control number.

1. REPORT DATE 07 APR 2004	2. REPORT TYPE N/A	3. DATES COVERED -	
4. TITLE AND SUBTITLE A comparison of the performance of 3 to 5 and 8 to 12 micrometer infrared cameras		5a. CONTRACT NUMBER	
		5b. GRANT NUMBER	
		5c. PROGRAM ELEMENT NUMBER	
6. AUTHOR(S) Thomas Meitzler; Grant Gerhart; Euijung Sohn; Paul Collins		5d. PROJECT NUMBER	
		5e. TASK NUMBER	
		5f. WORK UNIT NUMBER	
7. PERFORMING ORGANIZATION NAME(S) AND ADDRESS(ES) US Army RDECOM-TARDEC 6501 E 11 Mile Rd Warren, MI 48397-5000		8. PERFORMING ORGANIZATION REPORT NUMBER 18753	
9. SPONSORING/MONITORING AGENCY NAME(S) AND ADDRESS(ES)		10. SPONSOR/MONITOR'S ACRONYM(S) TACOM/TARDEC	
		11. SPONSOR/MONITOR'S REPORT NUMBER(S) 18753	
12. DISTRIBUTION/AVAILABILITY STATEMENT Approved for public release, distribution unlimited			
13. SUPPLEMENTARY NOTES Presented at SPIE 1994, Conference 2224, 7 April, 1994			
14. ABSTRACT			
15. SUBJECT TERMS			
16. SECURITY CLASSIFICATION OF:			17. LIMITATION OF ABSTRACT SAR
a. REPORT unclassified	b. ABSTRACT unclassified	c. THIS PAGE unclassified	
19a. NAME OF RESPONSIBLE PERSON			

Throughout this study, the authors were impressed by the scarcity of field data in adverse weather conditions for calibration and model verification. This just points to the need for such models as LOWTRAN, TTIM, etc. for reliable simulation purposes.

2. Simulation Methodology

In this paper, several parameters were used to assess the performance of sensors in the two IR bands. First, a comparative bandpass study was performed using a simulated AGEMA dual-band imager in conjunction with actual AGEMA dual-band field data. The purpose of this part was to get an idea of, everything else being equal, what is the best IR band (MW or LW) for remote sensing. The parameters that were varied were the target-to-sensor range, rain rate, and fog. Second, a traditional 8-12 micron scanning common module AN/TAS-4A (TOWII) FLIR sensor is compared to a late model 3.4-5.5 micron Sarnoff staring FPA sensor for a resolution comparison. Using the KRC field-data of the Bradley taken with the Agema, TTIM was used to resample and simulate the image of the TOWII and staring FPA. These field images include both 2.0-5.6 and 8-12 micron IR images from an AGEMA 900. The dual-band images were all taken at close range (< 1km) so long distance comparisons cannot be made. The scene containing the Bradley is ranged out to a few kilometers (km) to show the effects of range and the atmosphere on the image target. All the simulations of the sensor effects were done using the TARDEC Thermal Image Model (TTIM) which calls LOWTRAN7 for the modeling of atmospheric effects. The TTIM, LOWTRAN and MODTRAN calculations were all done on a Silicon Graphics workstation.

2.1 Description of Modeled Sensors

The following sensors were modeled in this study; a AN/TAS-4A 8-12 micron scanning array, an AGEMA 2.0 to 5.6 and 8-12 dual band scanning sensor, and a RCA Sarnoff 3.4 -5.5 staring focal plane array (FPA). The parameters for these sensors were found from specification sheets provided by the manufacturer and in the validation of TTIM paper by Engel⁹.

2.2 (3.4-5.5) Micron Staring FPA

The characteristics of the Sarnoff 3.4 -5.5 FPA are listed below in Table 1. The Sarnoff staring FPA is a late model FPA.

DAVID SARNOFF RESEARCH CENTER 640 x 640 PtSi FPA

Bandwidth	3.4 - 5.5 μm
Detector material	Platinum Silicide
I FOV (H,V)	0.48 mRad, 0.48 mRad
FOV (H,V)	390 mRad, 390 mRad
Detector area	$2.2 \times 10^{-6} \text{ cm}^2$
Pixel Size	24 x 24 microns
Focal length	500 mmeters
f/#	1.5
Channel type	Buried channel
Charge transfer efficiency	0.998
Frame rate	30 Hz
Fill factor	38%

Table 1

2.3 (8-12) Micron AN/TAS-4A

The TOW II scanning sensor is the common module FLIR. This is still the most fielded of all FLIR's. The properties of the TOW II are shown in Table 2 below.

THE AN/TAS-4A WFOV SCANNING IR SENSOR

Bandwidth	7.15 - 12.2 microns
IFOV (H,V)	0.4, 0.6 mRad
FOV (H,V)	119, 59 mRad
Detector area	$2.5 \times 10^{-5} \text{ cm}^2$
cut-on, cut-off frequency	$3, 5.1 \times 10^5$ (AC)
Scanning efficiency	1.00
Oversampling	Maximum along scan
Cross scan oversampling	1.2
Integration (along, cross)	1.0, .01
Frame rate	30 Hz

Table 2

2.4 AGEMA 900 DUAL BAND

The AGEMA dual band specifications are shown below in Table 3. the initial input images were taken with this camera.

specification	mediumwave	longwave
Bandpass	2.0 - 5.6	8 - 12
IFOV(H,V)	0.22 mRad	0.19 mRad
FOV(H,V)	44 x 22 mRad	44 x 22 mRad
cut-on, cut-off frequency	$0.5.1 \times 10^6$ (DC)	$3,5.1 \times 10^6$ (DC)
Detector type	InSb	HgCdTe
No. of Detectors	1	1
Scan Type	Two dimensional	Two dimensional
Interlace	1:4	1:4

Table 3

3. Comparison of MW and LW Cameras

3.1 Coupling and Sampling Considerations

The AN/TAS-4A is typical of first generation thermal imaging systems in that the signal processing is done by a series of AC coupled amplifiers. Second generation systems, such as the Sarnoff staring FPA usually use some form of DC restoration.^{9,10} One problem with TOWII imagery is the characteristic stripe across the image. Artifacts can be caused by: 1) scanning and interlace errors, 2) a gap between successive scan lines and 3) detector variations in the 60X1 linear array. The stripe is caused by the third, detector responsivity variations. TTIM simulates variations of the detectors within such an array by using a random detector sensitivity, or gain, with the variance specified by a user input parameter. In all the following images, the simulated views were enlarged to a standard size for better viewing. With the enlargement comes a certain amount of pixelation as the range from the target to the camera increases. Ordinarily the image becomes smaller as range increases.

The authors enlarged the image through replication to show MTF and sampling losses. In addition, for display purposes, the images were autoscaled for all cases. The authors found that if manual scaling from the shortest range on out was used the images become "washed out" at less than 1km.

3.2. Bandpass Comparison (AGEMA Dual-Band)

For the case of the AGEMA dual-band comparison refer to Figures 3a through 3d. In the case of a clear atmosphere, fig. 3a, the MW band is the clear winner. The contrast of the background is better and the overall target and image clarity of the MW band is better than the LW band. Under a heavy fog, figure 3b, the LW band is now producing a better image. The vehicle and background are barely visible in the MW band. Even the separate road wheels are visible at a distance of 0.4 km using the LW band. Figure 3c shows the same set of ranges under moderate and, in fig 3d, heavy rain conditions. In all image simulations the contrast was autoscaled, hence, the target appears to get brighter as range increases. If the images were manually scaled at each range, rather than autoscaled, the images were too dark to be of much use. For ranges less than 0.3 km the MW image shows better contrast, however, the MW band image quality decays quickly with range in the presence of rain. The plots in Figure 4 are the MODTRAN spectral plots of the transmittance versus wavelength. The average transmittance is less in the 3-5 band than in the 8-12 band. MODTRAN results are shown below in Table 5.

3.3 Resolution Comparison (TOW II and Sarnoff FPA)

For the resolution comparison the TOW II was compared with the Sarnoff staring FPA, see figures 2a through 2d. In figure 2a, are the simulations of the two cameras under clear atmosphere conditions, (23 km visibility). The Sarnoff FPA image has a better background contrast and also better internal textural and target feature resolution compared to the TOW II image out to a distance of about 1 km. The TOW II image is plagued by the strip artifact caused by the scanning/interlace errors and detector variations. The TOW II image is also less resolved (more blurry). Figure 2b shows the TTIM simulations under foggy conditions. Even at short range, in a foggy atmosphere, the TOW II image is slightly better than the Sarnoff FPA. As the range increases, the FPA image quickly degrades. After two hundred meters, the TOW II images are better even though they are more blurry and less background contrast and have the fixed pattern stripe. On figures 2c and 2d, the Sarnoff FPA and TOW II scanning array are compared in rainy conditions. Out to around .6 km the performance of the Sarnoff is still better than the TOW II. Beyond 0.6 km, the LW band image is better.

MODTRAN CALCULATIONS

The plots in Figure 4 are the MODTRAN spectral plots of the transmittance versus wavelength. The average transmittance in the 8-12 band is almost twice that in the 2.0-5.6 band. Water and carbon dioxide have pronounced absorption lines in the 2.0-5.6 band. MODTRAN results are shown below in Table 5.

wavelength (microns)	condition	Range (km)	ave transmittance
2-5.6	clear	2	0.5220
2-5.6	heavy rain	2	0.0137
8-12	clear	2	0.8606
8-12	heavy rain	2	0.0229

Table 5

4. Conclusions

For general purpose, all-weather viewing conditions, the LW band was again shown to be the best band in terms of least degradation to the image quality by atmospheric water and carbon-dioxide absorption. What was interesting was how well late model staring FPA's can do out to a certain range and in the presence of rain. The Sarnoff staring array (MW FPA) had a better resolution than the TOWII

or Agema in every case except fog for ranges under 1.5 km. The MW band has large absorption peaks due water and carbon dioxide which will always cause problems for detection ranges. On the other hand, for clear atmospheres and short ranges, the preference may be in using a late model scanning or staring FPA because of their excellent resolution and contrast capability. The utility of a suite of models such as TTIM was also shown. Taking field data is expensive and having the capability to resample data taken with other cameras or systems for further simulation is very useful.

5. Future Study

Recently the authors have begun work on a Cooperative Research and Development Agreement (CRADA) with FORD Motor Co. to investigate the automotive vision enhancement capabilities of thermal systems. The goal of the CRADA is to model several existing and novel sensor architectures as well as IR bands for possible use in future automotive applications. Of particular interest is to compare the near-IR (SW) bands with the MW and LW.

6. Acknowledgments

The authors appreciate the field images on tape that Mr. John D'Agostino and Mr. John Palmer had sent from the Night Vision Labs. Thanks are extended to Mr. Jim Chetwynd of the AFGL for instruction on some fine points to using MODTRAN and Mr. Dave Tofsted of BED for help in the rain extinction coefficients. The authors also extend their thanks to Mr. Paul Rogers of TARDEC for the sharing with them of the KRC dual-band data reports.

7. References

1. T.W. Tauer, "Thermal Imaging Systems' Relative Performance:3-5 micron vs. 8-12 micron," AFAL-TR-76-217, AF Avionics Lab, WPAFB, OH, Jan. 1977.
2. A.F. Milton, G.L. Harvey, and A.W. Schmidt, "Comparison of the 3-5 micron and 8-12 micron Regions for Advanced Thermal Imaging Systems:LOWTRAN Revisited," NRL Report 8172, NRL, Washington, DC, Dec. 1977.
3. T. Jaeger, A. Nordbryhn, RA Stokeseth, "Detection of Low Contrast Targets at 5 micron and 10 micron: a comparison," Appl. Optics, 11, 1833-1835, 1972.
4. R. Longshore, P. Raimondi and M. Lumpkin, "Selection of Detector Peak Wavelength for Optimum Infrared System Performance," Infrared Physics, 16, 639-647, 1976.
5. J. Williams, 'Infrared Transmission and Path Radiance Through Dust and Fog," ARL-MR-35, April 1993.
6. F.Y. Kneizys, J.H. Chetwynd, et al., "Atmospheric Transmittance/Radiance:LOWTRAN5," AFGL-TR-80-0067, AFGL, Hanscom AFB, MA, Feb. 1980.
7. T. Rogne, T. Cook, R. Freeling, TTIM Reference Manual, OMI Report.
8. J. Ratches, et al., "Night Vision Lab Static Performance Model For Thermal Viewing Systems," ECOM-7043, April 1975.
9. M. Engel and Y. Bushlin, "Field Test Validation of the TTIM Sensor Model:Results of Comparison with a Real Sensor," EO R&D Div., Technion R&D Foundation, Technion City, Haifa, Israel.
10. H. Kennedy, "Modeling second-generation thermal imaging systems," Optical Eng., Nov. 1991, Vol. 30, No. 11, pp. 1771-1778.

SCHEMATIC REPRESENTATION OF SCANNING SENSOR STRUCTURE

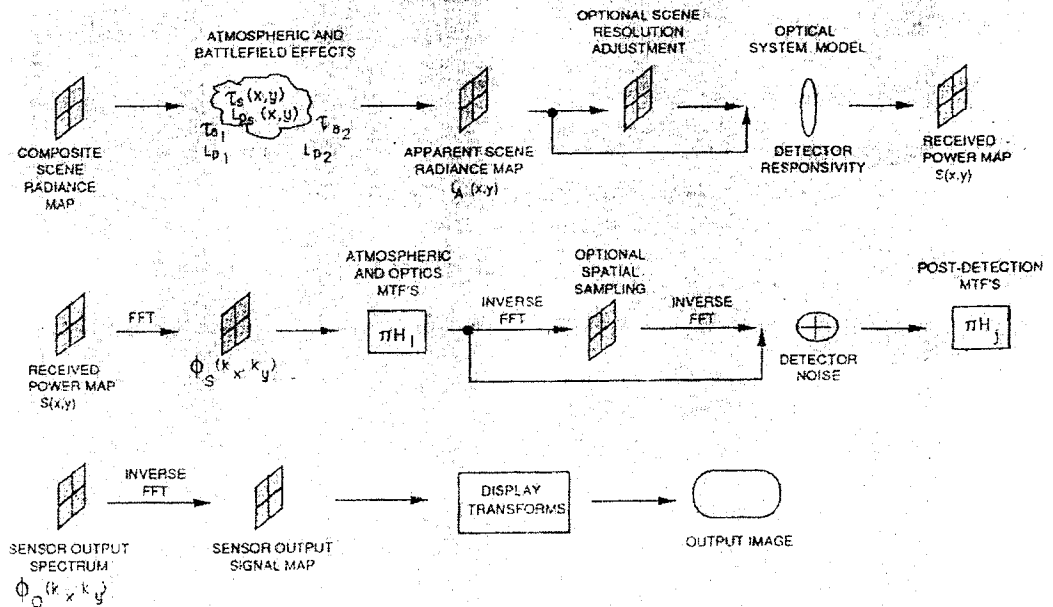


Fig 1

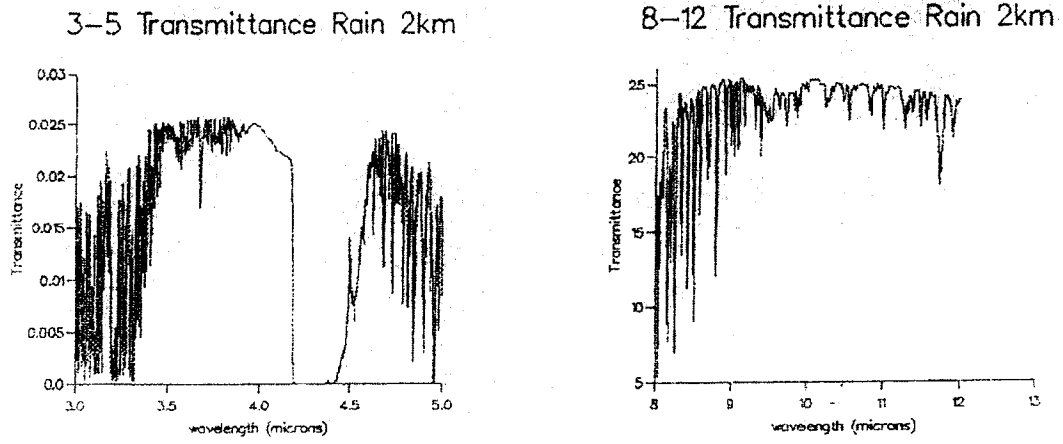


Fig 4

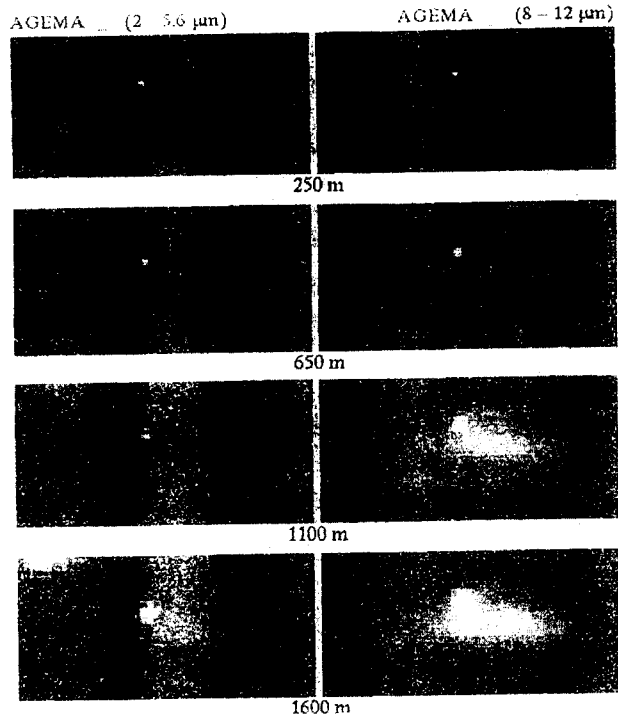


Figure 3(a)

Figure 3(c)

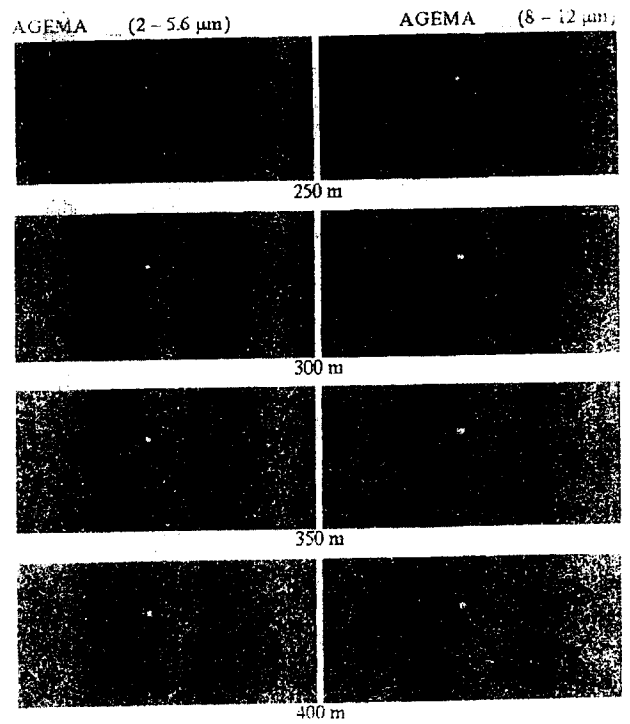
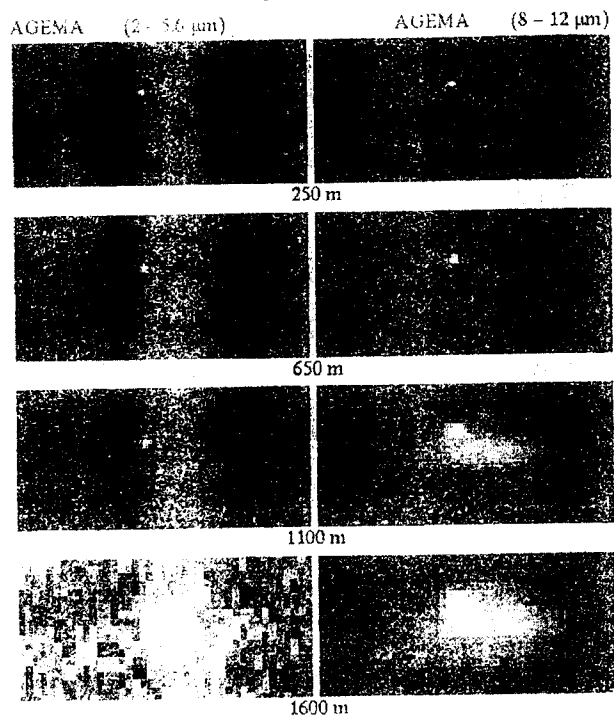
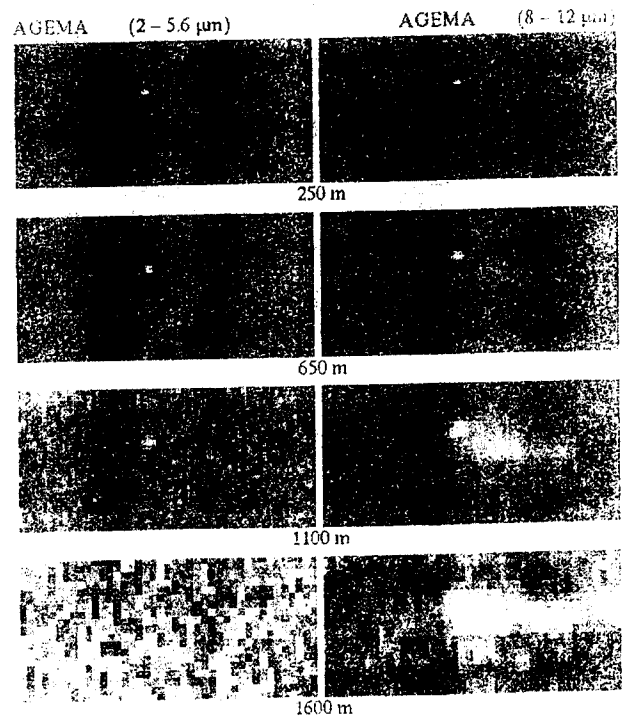


Figure 3(b)

Figure 3(d)



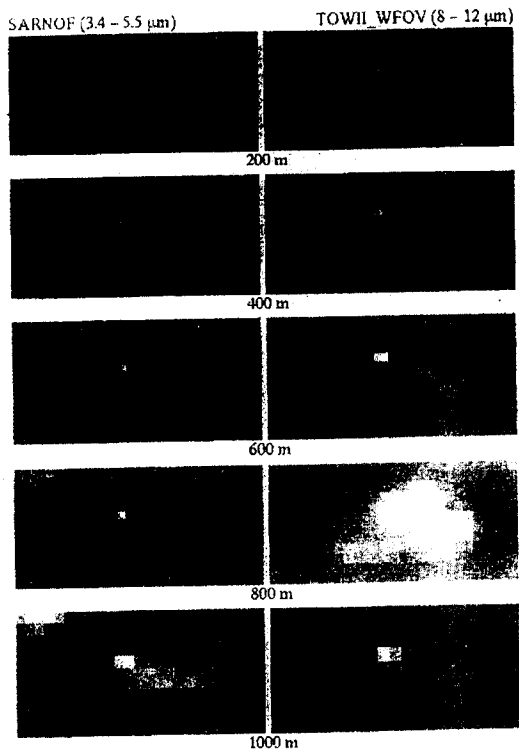


Figure 2(a)

Figure 2(c)

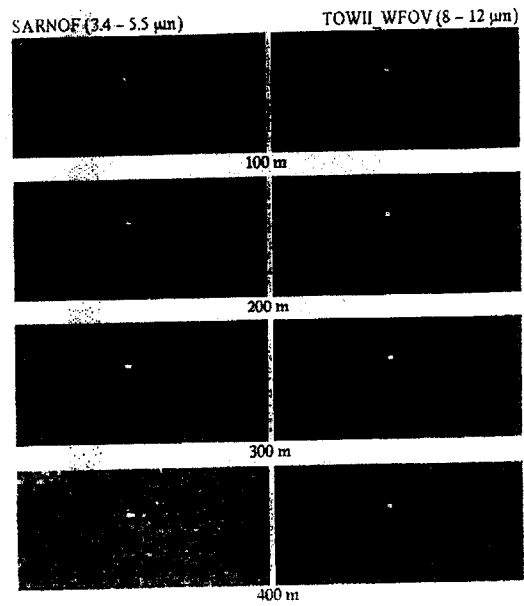
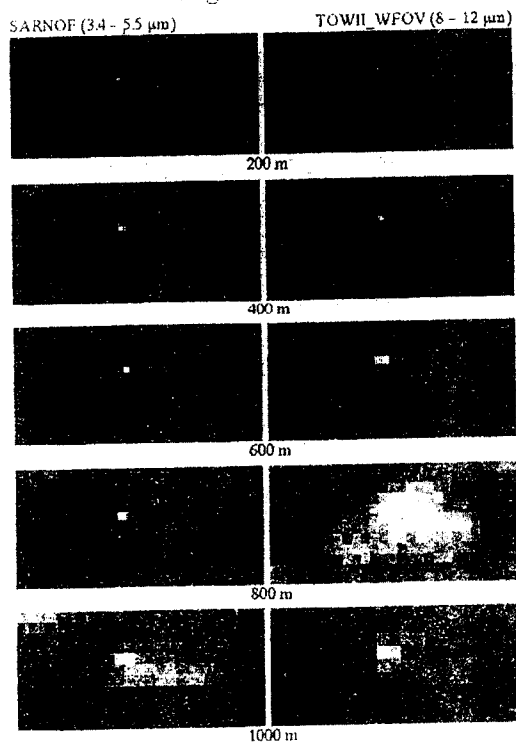


Figure 2(b)

Figure 2(d)

